Hindawi
Geofluids
Volume 2021, Article ID 6639383, 12 pages
https://doi.org/10.1155/2021/6639383

Research Article

Experimental Investigation on Frost Heaving Force (FHF) Evolution in Preflawed Rocks Exposed to Cyclic Freeze-Thaw Conditions

Yu Wang, Tao Sun, Haonan Yang, Jinfeng Lin, and Hao Liu

Beijing Key Laboratory of Urban Underground Space Engineering, Department of Civil Engineering, School of Civil & Resource Engineering, University of Science & Technology Beijing, Beijing 100083, China

Correspondence should be addressed to Yu Wang; wyzhou@ustb.edu.cn

Received 16 December 2020; Revised 10 January 2021; Accepted 19 January 2021; Published 3 February 2021

Academic Editor: Feng Xiong

This work is aimed at investigating the structural deterioration and the frost heaving force evolution characteristics of flawed rocks using a self-developed frost heaving force (FHF) measurement system. Three kinds of preflawed rocks with different flaw geometry parameters were used to conduct the FHF measurement tests. The testing results reveal five distinguished stages from the frost heaving force evolution curve; they are the inoculation stage, explosive stage, decline to steady stage, recovery stage, and sudden drop stage. In addition, a secondary frost heaving phenomenon is found, and the secondary peak value is lower than the initial peak value. Moreover, the FHF decreases with increasing the F-T cycle number, and its decreasing rate becomes faster at a high F-T cycle. The frost heaving force is affected not only by flaw geometry but also by the lithology. For low-pore hard rock, damage propagates quickly after the occurrence of freeze-thaw damage. It is suggested that the mesoscopic structure of rock affects the water migration and water-ice phase transformation, and rock can be fractured by FHF in the preexisting flaws.

1. Introduction

In cold regions, the freeze-thaw (F-T) actions within the preexisting discontinuous (e.g., bedding planes, interbeds, cracks, foliation, flaw, and fault) would lead to the instability and damage of rock, such as avalanche, collapses, rock falling, and landslides [1–6]. Water from the thawing of snow or sleet penetrates those rock discontinuities, and freeze occurs when the temperature is below zero and the frost heaving force produces within the preexisting fractures or discontinuities. The frost heaving force drives the propagation of the geological discontinuities, resulting in the increment of fracture aperture and length and deterioration of the rock structure [4]. Ice-driven mechanical weathering is generally considered to be a crucial process that impacts the long-term stability of rock mass. For example, frost heaving force induced by frost heave of surrounding rock in cold region tunnels or mines could result in lining cracking, water leakage, and drain blockage with ice, which seriously affects the normal operation. Therefore, investigation on the evolution of FHF and especially the cyclic freeze-thaw evolution of FHF is crucial to reveal the structural deterioration mechanism of rock mass.

After detailed literature review, many studies have been conducted on the evolution of frost heaving force, including theoretical, experimental, and field investigations. Some scholars measured the frost heaving force by ice extrusion in open flaws, and it is from 0 to 7 MPa. This finding has also been proved from field investigation [7]. Winkler [8] obtained the expansion forces of pore ice in rock pores at −5°C, −10°C, and −22°C, respectively, and they pointed out that the frost heaving force by pore water freezing can reach tens to hundreds of megapascal. Akagawa and Fukuda [9] proposed a theoretical equation to calculate the frost heaving force by segregation freezing theory. Arosio et al. [10] used a thin film pressure sensor to test the frost heaving force of the preflawed rock samples after water filling, and the maximum frost heaving force was up to 5 MPa. Davidson and Nye [11] measured the maximum frost heaving force of the saturated crack with a width of 1 mm in a transparent material by a

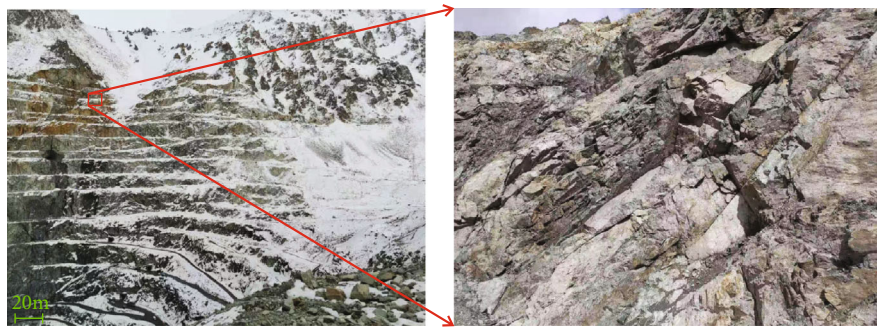

(a) (b)

Figure 1: Description of the rock mass structural characteristics in the eastern open pit slope of Beizhan iron mine. An obvious rock bridge structure can be observed from the outcrop.

photoelastic test and found that the frost heaving force was 1.1 MPa. Lin et al. [12] established a 3D joint frost heaving force model under cyclic freeze-thaw conditions; the destitution of the FHF within the natural fractures was obtained. Their model found that the FHF decreases with the freeze-thaw cycle significantly. Bost and Pouya [13] presented an assessment method for the stress generated by freezing in open rock cracks. Huang et al. [14] preformed frost heaving measurement experiments in rock-like material by using a thin film pressure sensor, and they found that the FHF is about 1.5 to 7.2 MPa for a single flaw. An empirical equation was proposed by Lv et al. [15] to describe the variation of frost heaving deformation, and the maximum FHF was estimated. Zhang et al. [16] introduced the fracture mechanics to calculate the frost heaving force; they pointed out that pure mode-I fracture occurred resulting from the frost heaving force. They found that the rock elastic parameter of Poisson's ratio and elastic modulus and the equivalent volume expansion coefficient of water-ice medium influenced the frost heaving force. Wang et al. [17] measured the frost heaving force in preflawed granite and found that F-T damage increased with the F-T cycle, and the FHF decreases with increasing the F-T cycle. Plenty of experimental methods have been conducted on flawed or notched rock subjected to freeze-thaw treatment, and the potential FHF was obtained. Although some interesting findings have been revealed from the above experiments, almost all the FHF measurement is different; experiments on notched limestone specimens submitted to freeze-thaw cycles were performed. The above studies have made abundant achievements, mainly focusing on the evolution of frost heaving force under one freeze-thaw cycle, while few studies focus on the frost heaving force evolution under cyclic freeze-thaw cycles. In fact, the engineering rocks in cold regions are subjected to repeated freeze-thaw actions, and the changes of frost heaving force with the freeze-thaw cycle can help us to understand the structural deterioration mechanism of naturally fractured rock mass.

It is accepted that the frost heaving force is impacted by many factors, such as geometry of the flaws [18, 19], rock saturation degree [20], thermodynamic parameters [21, 22], rock mechanical parameters [23], and freezing direction [24]. Among many of the factors, lithology and flaw geometric shape influence a lot to frost heaving force. Therefore, this work focuses on the cyclic frost heaving deterioration characteristics of rock mass considering the rock type and the flaw width and length. The evolution characteristics of peak frost heaving force with the freeze-thaw cycle are firstly discussed for three kinds of rocks, i.e., marble, granite, and sandstone.

2. Materials and Methods

2.1. Rock Material Descriptions. The studied rock material was obtained from a high-altitude alpine mining in Hejing Beizhan open pit slope located at the Xinjiang province, northwest of China (Figure 1(a)). The mining area is 123 km away from the Hejing County in the direction of 327°; the straight-line distance is 84 km away from Baluntai town of Hejing County, as shown in Figure 1. The mining area is located near the main ridge of Tianshan mountain on the north slope of Boluo Huoluo Mountain. The mountain trend is nearly east-west, and the overall terrain is high in the south and low in the north, with an altitude of 3,160~4,575 m and a relative altitude of 700~1000 m. The orebody is located at an altitude of 3450~3723 m. The mining area belongs to continental temperate semiarid climate, which is a cold-climate zone with snow all year round in high mountains (Figure 1(b)). Over the years, the average temperature of January to April and September to December is below zero, with the lowest temperature reaching -40°C.

As is proved by the previous studies, the mesoscopic structure of rock is obviously related to the frost heaving force; therefore, SEM observation was performed to reveal the mesoscopic structure of the tested rock samples. For the sandstone, it is obvious that its porosity is much more than that of the marble and granite; the pore structure can be observed by the naked eye. Therefore, SEM testing was not carried out on the sandstone, and we only observe the mesoscopic structure of the marble and granite samples, as shown in Figure 2. It is shown that the porosity of marble is obviously lower than that of the granite; therefore, the texture of marble presents strong compactness. It can be speculated that the densification of marble is the largest among the three kinds of rock. After performing basic physical and mechanical testing, the density of the marble, granite, and sandstone is 2.75, 2.55, and 2.35 g/cm^3, respectively. The porosity of

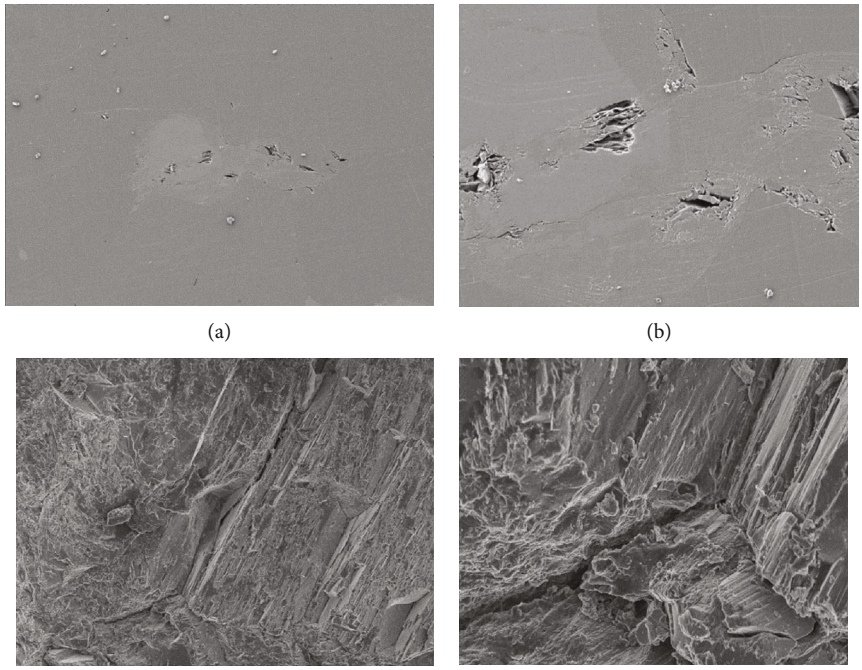

(a) (b)

(c) (d)

Figure 2: SEM results of different magnifications for marble and granite: (a, b) results of 500 and 2000 times magnification of marble, respectively; (c, d) results of 500 and 2000 times magnification of monzonite porphyry, respectively.

(a) (b)

Figure 3: Preparation of rock sample with preexisting flaws: (a) the water-jet machine; (b) rock samples of different lithology with flaws used in the test.

them is 0.5%, 2.5%, and 16%, respectively. The uniaxial compressive strength of them is 225.51, 171.31, and 126.03 MPa, respectively. Because the peak frost heaving force is strongly related to rock tensile strength, the Brazilian splitting test was carried out to obtain the tensile strength of rock, and they are 23.03, 18.52, and 11.45 MPa, respectively.

Three typical rocks of marble, granite, and sandstone were prepared to conduct the frost heaving force measurement testing. The tested rocks were cored to a diameter of 50 mm and ground flat and parallel within ±0.1 mm to a nominal length of 100 mm according to the ISRM suggested method [25]. In order to mimic the open-typed natural fractures and ensure to reduce the effects of rock lithology on the experimental results, three preflaws were prepared using a water-jet system (Figure 3(a)) within each cylindrical rock core. The mixture of high-pressure water with garnet abrasive from a 0.75 mm, 1.5 mm, and 2 mm diameter nozzle produced a defect with an aperture of 1 mm, 2 mm, and 3 mm, respectively. The geometric morphology of the treble-flaw sample is a combination of three horizontal flaws with a length of 12 mm, 24 mm, and 36 mm. For rock with the same lithology, the flaw width is set to be 1 mm, 2 mm, and 3 mm, respectively. From the outcrop of the rock mass in the open pit slope, it can be seen that the natural fractures almost all present as an opening state due to the disturbance of blasting vibration; therefore, in this work, the flaws inside the rocks

were prepared as an open state with no cement material. The prepared samples are shown in Figure 3(b).

2.2. Testing Device and Method. After the preparation of pre-flawed samples, the rock samples were treated with vacuum saturation treatment for 24 hours with a vacuum saturation apparatus (Figure 4) and then treated with an F-T cycle. It is proved that it took 2.5 hours to realize one F-T cycle; the F-T scheme is shown in Figure 5. A specially self-developed frost heaving measurement system is used to monitor the evolution of frost heaving force, as shown in Figure 6. The system is composed of an ultralow temperature freezer, a film pressure sensor, a frost heaving force recording software, a date acquisition card, and a temperature-humidity controller. The film pressure sensor is the core component of the system. Its type is FSR402 made by Interlink Electronics, Inc. The size of the sensor is 5 mm in diameter and 38 mm in length. The sensor is a kind of robust polymer thick film (PTF) device that exhibits a decrease in resistance with an increase in force applied to the surface of the sensor. The actuation force is 0.2 N, the force sensitivity range is 0.2 N~20 N, and the operating temperature performance is cold -40°C and hot 85°C. The recording frequency of the data acquisition system is 5 Hz, and the range of the temperature recorder is -200°C~80°C. It is equipped with a waterproof metal probe with an accuracy of ±0.2°C, and the data acquisition frequency is 1/60 Hz. According to the temperature change of the open pit mine slope, the saturated samples were put into the freezer apparatus and under −30°C; then, the samples were taken out of the freezer and allowed to thaw; by doing so, a freeze-thaw cycle is realized and the frost heaving force is monitored at the same time.

2.3. Testing Procedure. The detailed testing procedures are summarized as below:

(1) The temperature of the digital controlled ultralow temperature freezer was set to -40°C in advance, the waterproof treatment method was carried out to the thin film sensor, and then, its working condition was checked again. The saturated rock samples with preexisting flaws were taken out of the vacuum saturation apparatus

(2) Connecting the frost heaving force test system, at the same time, a temperature test system is installed in the flaws of the rock sample. Afterwards, the pure water was injected into the crack with a syringe and put into the refrigerator, and the monitoring system was started simultaneously. Three flaws were conducted frost heaving force measurement in the same sample for each testing

(3) The freeze heaving force evolution within a F-T cycle was recorded. We observed the change of the FHF curve and the measurement continuously until the FHF reaches a minimum. Afterwards, multiple freeze-thaw cycles were applied to the rock sample

Figure 4: The vacuum saturation apparatus.

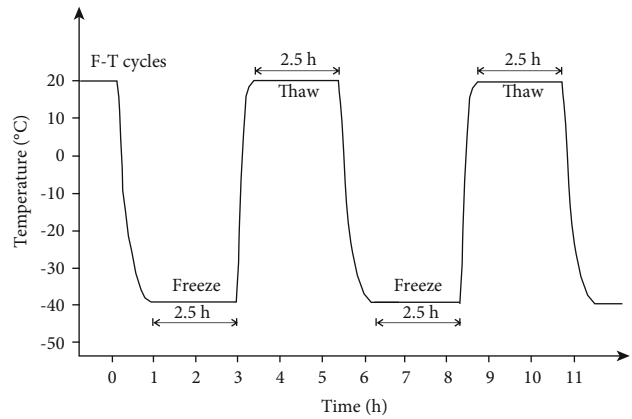

Figure 5: The cyclic F-T scheme in this work.

(4) Repeating the above experimental steps, all the samples are tested to get the FHF evolution and its peak stress

3. Results and Discussions

3.1. FHF Evolution in a Single F-T Cycle. Using the FHF measurement system, the FHF evolution curves for rock with different lithology and flaw geometry are shown in Figure 7. It is shown that the evolution pattern of the FHF curve is similar for different tested samples; the evolution characteristics are not influenced by the rock type and flaw geometric structure. The changes of the FHF experience five obvious stages; they are the inoculation stage, explosion stage, decline to steady stage, recovery stage, and sudden drop stage. The FHF characteristics for each stage are described in detail as below:

(1) *Frost Heaving Force Inoculation Stage*. In this stage, temperature gradually dropped below zero, but frost heaving force does not generate in the flaws. Although the temperature dropped below zero, the water itself is stored with certain heat; in this stage, the water in flaws still releases heat energy until the temperature dropped to -5°C or so later. When freeze

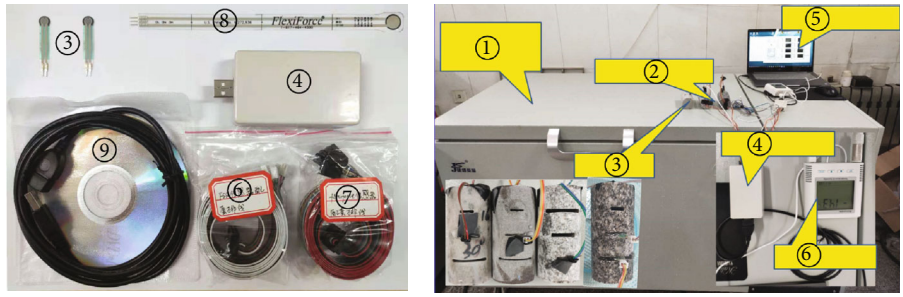

(a) (b)

Figure 6: The self-developed frost heaving force measurement device: (a) component of the frost heaving measurement device; (b) FHF measurement system: 1: ultralow temperature freeze-thaw environment box; 2: film pressure sensor of FSR-400; 3: rock sample with preexisting flaws; 4: frost heaving force acquisition card; 5: frost heaving force recording software; 6: temperature-humidity collector; 7: Flexible Flat Cable of FSR 200; 8: film pressure sensor of Flexifore 201; 9: data transmission cable; 10: Flexible Flat Cable of Flexifore 201.

occurs, the openness segment of flaw first freezes, resulting in the formation of an icy surface. Due to the ice jam effect, the flaw is in a closed system. Although a 9% volume expansion occurs when water transfers to ice, frost heaving force does not occur at this stage

(2) *Explosion Stage*. As the temperature decreases, the freezing degree of the sample increases, and the water-ice phase transformation continues; this leads to volume expansion constant in the crack. Due to the boundary limitation of the flaw wall, the frost heaving force of the flaw increases constantly. As can be seen from Figure 5(a), the maximum frost heaving force for the flaw (granite, FW = 2 mm, FL = 24 mm, no cementation) reaches 5.85 MPa

(3) *Decline to Steady Stage*. At this stage, the temperature continues to decrease, but the frost heaving force does not increase continuously. Instead, the frost heaving force falls and gradually becomes stable. This is because when the frost heaving force exceeds the tensile strength of the rock matrix, damage occurs at the flaw tips resulting in the dissipation of frost heaving force. In this stage, the new cracks generate at the flaw tips and rock structure deteriorates accordingly

(4) *FHF Recovery Stage*. When the frost heaving force gets to the stable state, the rock sample was taken out of the ultralow temperature freezer. Ice in the flaws begin to thaw, and it can be seen that frost heaving force increases as the temperature rises gradually, and a secondary frost heave phenomenon occurs; frost heaving force curves present a peak point. After formation of the ice lens, frost heaving force sharply increases within a short time. Damage in the flaw tips leads to the decreasing of frost heaving force. The secondary frost heaving force is less than the first value, indicating that frost heaving damage occurs within the cracks

(5) *Sudden Drop Stage*. At this point, all the ice within the flaw melts, and the frost heaving force caused by the secondary frost heaving gradually dissipates. Thus, the rock frost heaving damage caused by the frost heaving force terminates. To summarize the evolution process of frost heaving force, it is found that the peak value of initial frost heaving force is the maximum force that can be sustained when flaw damage occurs. Therefore, the peak value of initial frost heaving force can be used to characterize the capacity of resistance to frost heaving for fractured rock mass

3.2. FHF Evolution during Cyclic F-T Treatment. The freeze-thaw as a typical fatigue loading acting on rock mass is frequently in cold regions. The rock structure would deteriorate when exposed to repeated freeze-thaw cycles. Actually, the deterioration of rock mechanical properties is caused by multiple freeze-thaw cycles and not only one freeze-thaw cycle. In this section, the cyclic FHF testings were studied to reveal the fatigue deterioration characteristics of rock. The FHF evolution curves of different rock types are plotted in Figure 8, a total of six F-T cycles are performed, and about 23 hours was needed to realize a whole test. Figures 9(a)–9(c) show the evolution of FHF with experimental time for the marble with $d = 3$ mm, $L = 36$ mm; $d = 2$ mm, $L = 24$ mm; and $d = 1$ mm, $L = 12$ mm, respectively. The results show that the peak FHF decreases with the increase of the F-T cycle; in addition, the secondary FHF also presents a decreasing trend as the F-T cycle grows. These results indicate the deterioration of the rock structure with increasing F-T treatment. In order to further reveal the effect of rock lithology on the initial peak FHF, Figure 9(d) plots the relationship between the peak FHF and F-T cycles. The equation fitting approach is used to investigate their relationship; the equation that has the highest correlation coefficient is determined as the final fitting equation. A power function is used to describe the relationship between the frost heaving force and the F-T cycle for the marble, granite, and sandstone samples. The fitting results indicate that the initial peak FHF decreases with increasing the F-T cycle, and the decreasing rate gets faster under high F-T treatment. In addition, the FHF is also influenced by the rock lithology, FHF for marble is the largest, and it is the minimum for the sandstone. This

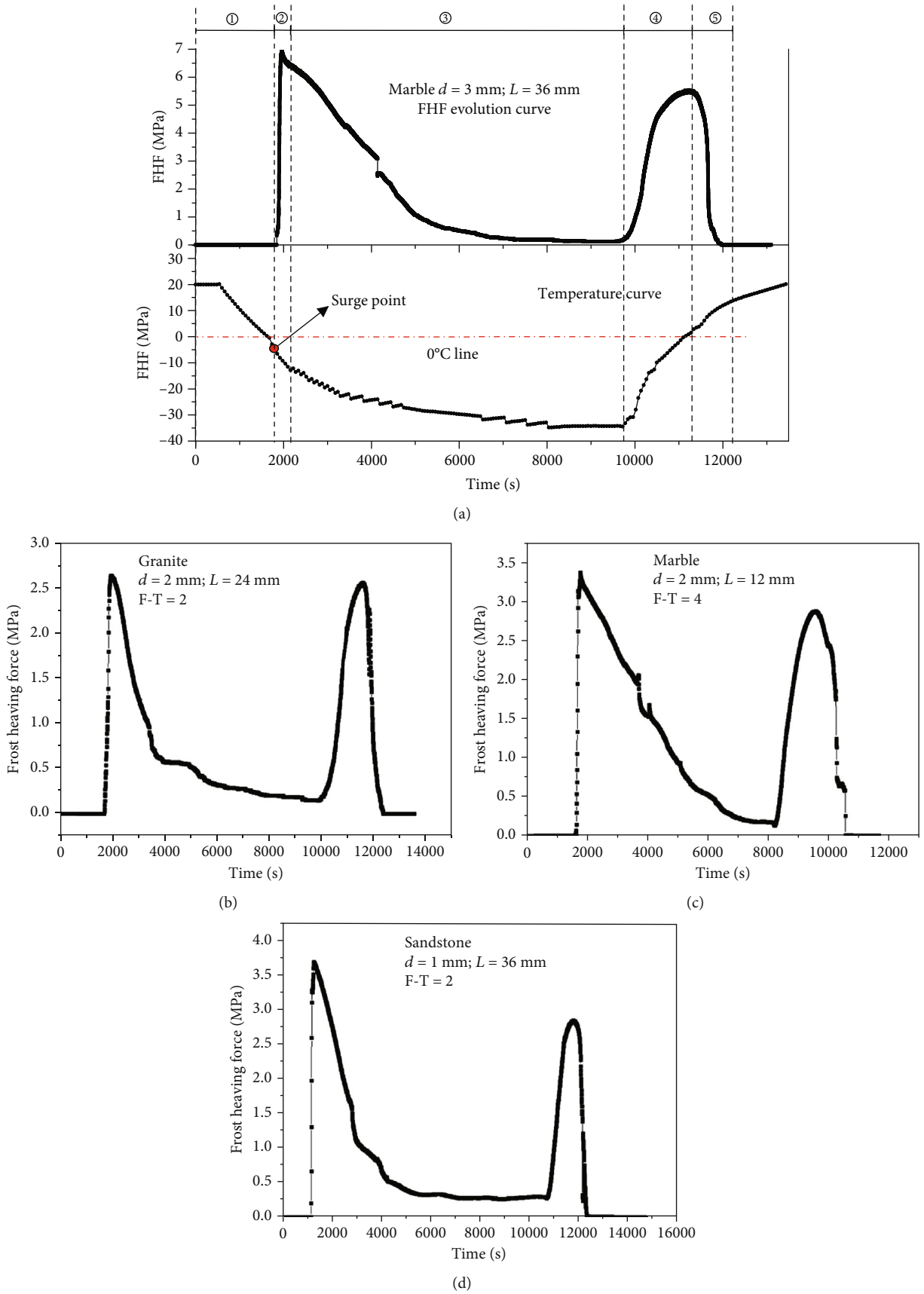

Figure 7: Typical FHF evolution curve during one F-T cycle, five obvious steps of FHF evolution can be observed.

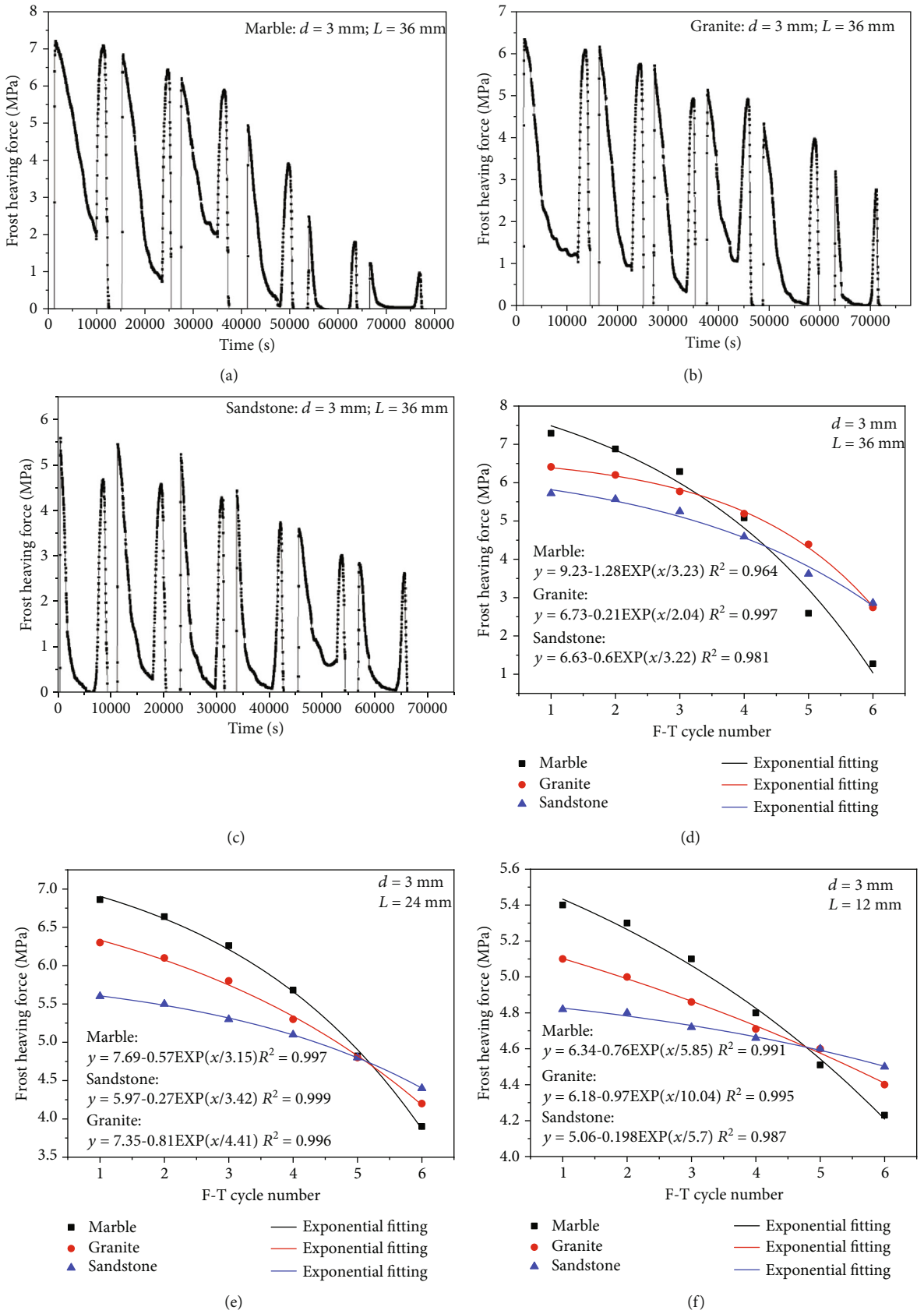

Figure 8: Duration curves of frost heaving pressure in different lithology: (a) marble; (b) monzonite porphyry; (c) sandstone. Relationship between initial frost heaving pressure and freeze-thaw times: (d) $d = 3$ mm, $L = 36$ mm; (e) $d = 2$ mm, $L = 24$ mm; (f) $d = 1$ mm, $L = 12$ mm.

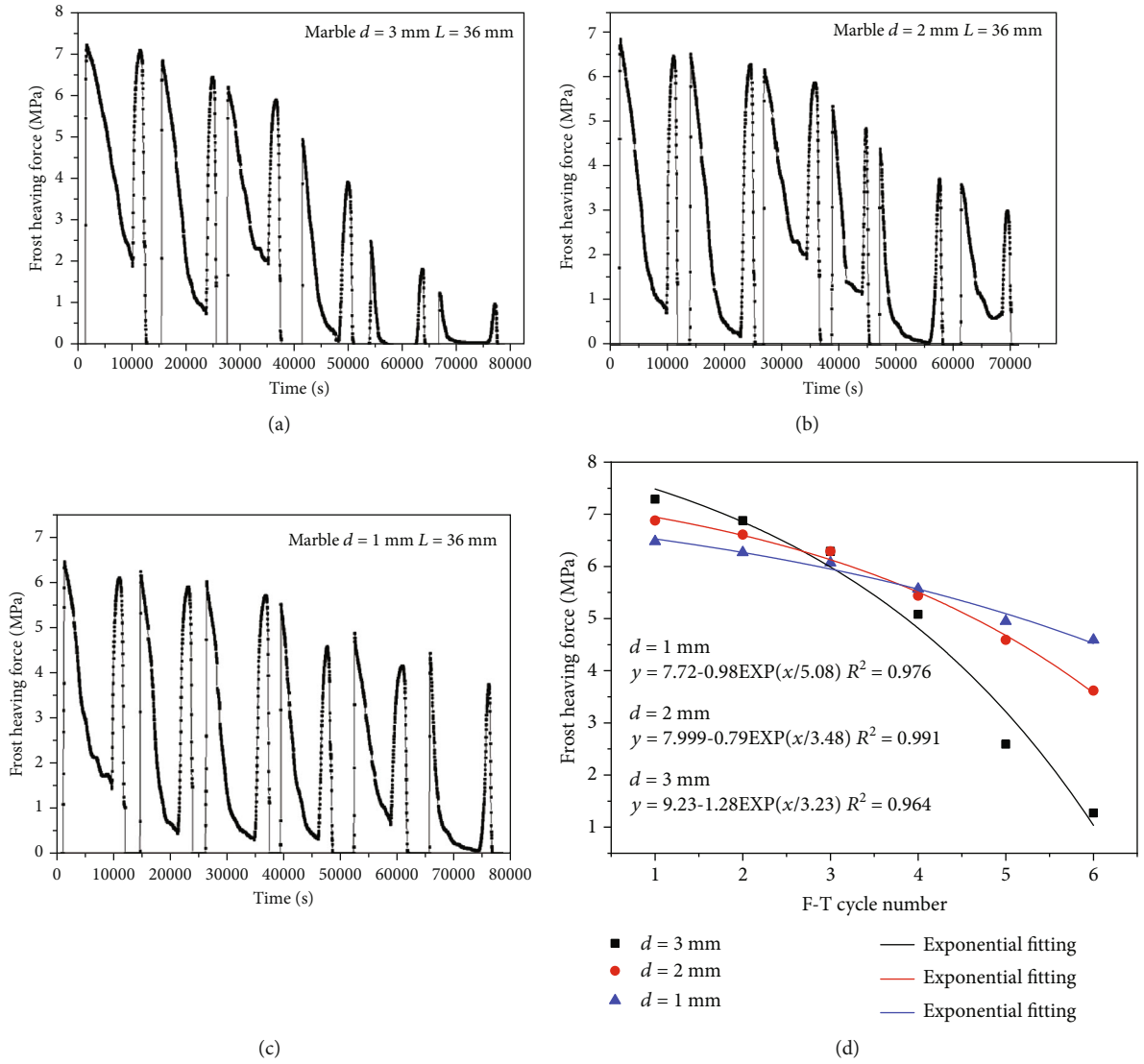

Figure 9: Optimal combinations to maximize the frost heaving force: (a–d) plots of the optimal factors of flaw width, flaw length, flaw cement type, and rock lithology, respectively.

result further proves the fact that the mesoscopic structure of rock has a direct impact on the FHF evolution characteristics.

As analyzed above, after the peak FHF, for rock under thawing treatment, the frost heaving force gradually increases again, and a secondary freeze-thaw phenomenon is found. We also studied the relationship among the initial FHF peak, secondary FHF value, and the F-T cycle, as shown in Figure 10. In Figure 10(a), the results also show that the secondary FHF decreases with increasing the F-T cycle. Due to the difference in rock lithology, the decreasing trend for the three types of rock is different, and the decreasing rate of marble is the largest (see Figure 10(b)). The result indicates that the damage propagation rate is higher for marble than granite and sandstone under tensile stress condition. The brittleness of marble is relatively high; the crack propagation rate is higher for marble than granite and sandstone.

3.3. Effect of Flaw Geometry Pattern on FHF Characteristics. Taking the marble, for example, the influence of the flaw length on FHF evolution is plotted in Figure 11. It can be seen that the FHF evolution characteristics are impacted by the preexisting flaw length. For the first several F-T cycles, FHF increases with the increase of flaw length; however, it decreases after several F-T cycles. This result indicates that the accumulated damage caused by F-T is larger for rock with longer flaws. For rock with a longer flaw, the tensile stress on the flaw tip is relatively large; accumulated damage occurs during repeated F-T treatment. The ability of rock to resist tensile stress becomes weaker, and this results in the sharp decrement of FHF at a high F-T cycle. The relationship between the FHF and the F-T cycle is shown in Figure 9(d), the power function is used to fit their relations, and we can see that the decreasing rate becomes faster at a high F-T cycle.

The impact of the flaw width on FHF evolution is also studied, as shown in Figure 9. The similar changing trend can also be observed from the evolution of FHF with the experimental time. The initial and secondary peak values of

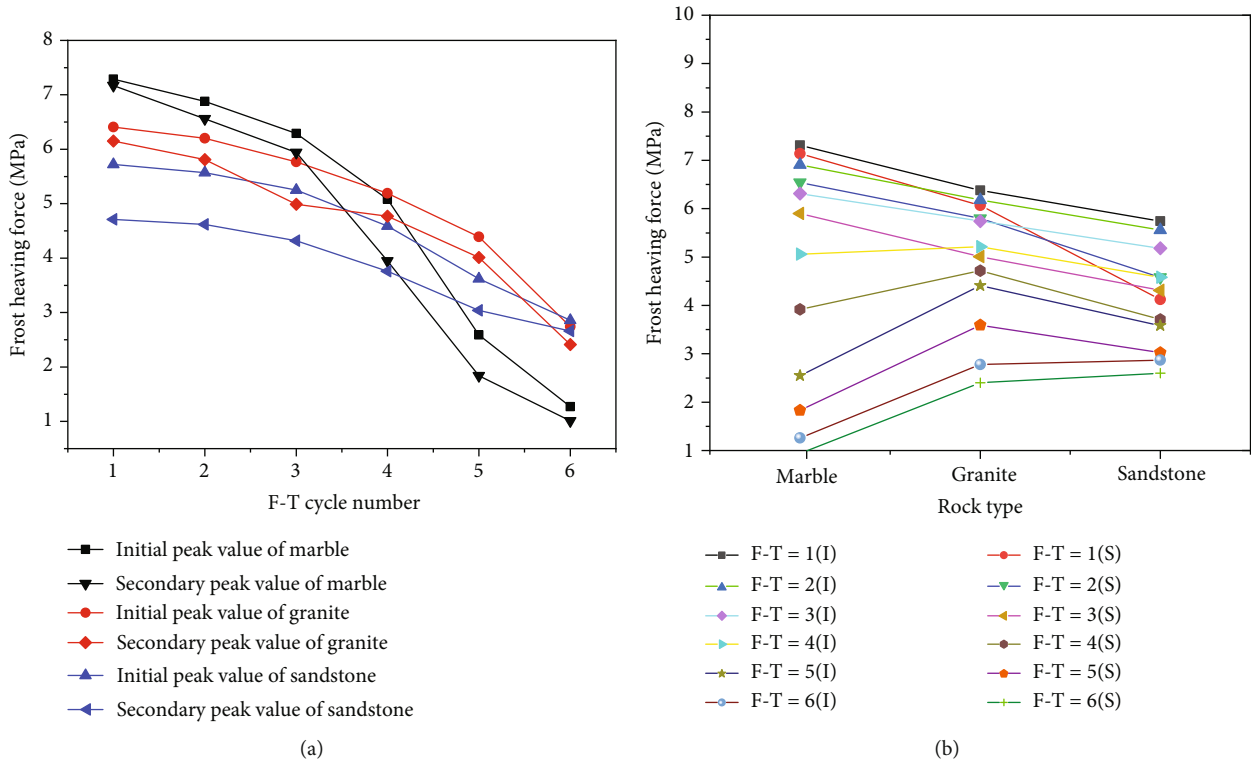

Figure 10: Plots of the influence of rock lithology on frost heaving force evolution characteristics: (a) change of the initial FHF, secondary FHF with F-T cycle number; (b) comparison of the frost heaving force for rock with different lithology.

FHF both decrease with increasing the F-T cycle, and the decreasing rate becomes faster for rock subjected to high F-T treatment. The influence of flaw width on FHF is attributed to the influence of flaw volume on FHF. Both the flaw width and length influence the peak value of FHF. Since the evolution law of FHF during the cyclic freeze-thaw process in different flaw lengths can also be applied to different flaw widths, more discussion and analysis are not stated here.

By analyzing the evolution law of frost heave force under cyclic freeze-thaw condition, it is found that the influence of the flaw length and width on the FHF evolution law is basically the same, and it is concluded that the main factor affecting the evolution law of FHF is the flaw volume inside rock samples. Due to the large volume of flaw expansion and large water storage, larger FHF is easy to be accumulated during the freezing process. Meanwhile, rock mass with large fracture expansion has a weak ability to resist frost heaving damage. Therefore, after repeated freeze-thaw cycles, the more developed the natural fractures in rock mass are, the more severe the frost heaving damage will be.

4. Discussions

The influences of the lithology and flaw geometry on the FHF evolution in the preexisting rock samples exposed to cyclic freeze-thaw are discussed in the above experiments. Under the action of multiple freeze-thaw cycles, the evolution of FHF in each cycle still experiences five stages, namely, incubation, explosion, stable fall, recovery, and dissipation. The repeated frost heaving action results in the damage accumulation inside flaws and would further affect the FHF evolution. During this period, the FHF is continuously incubated, released, and dissipated, causing fatigue damage of fractured rock mass. In the freezing process, due to the thermal energy of water in the flaws, the water at the fissure opening takes the lead in freezing to form the ice-blocking effect until the temperature drops to about -5°C, which makes the flaw become a closed system. The water-ice phase transformation in the flaws further results in the occurrence of frost heaving water pressure and volume expansion pressure of the unfrozen flaw water, as shown in Figure 12(a). In the thawing process, a secondary FHF peak can also be observed from the FHF evolution curve. The reason for this phenomenon may be attributed to the differential thawing of ice at the openness and within the flaws. The ice lens first melts for the openness partition; afterwards, the melt water migrates down gradually, and the temperature of the flaw central is still low and a lot of ice exists, as shown in Figure 12(b). As a result, the upper melt water freezes into ice again, leading to the phenomenon of secondary frost heave. However, the secondary frost heaving force is smaller than the initial frost heaving force. This is related to the previous damage of the flaw tip; the accumulated stress in the tips decreases after the previous damage. After a repeated freeze-thaw cycle, when the frost heaving force exceeds the tensile stress of the rock sample, a cracking phenomenon occurs. Obvious cracks can be observed from the rock surface (see Figure 13).

From the evolution of FHF during several F-T cycles, it is shown that the initial peak FHF and the secondary peak FHF

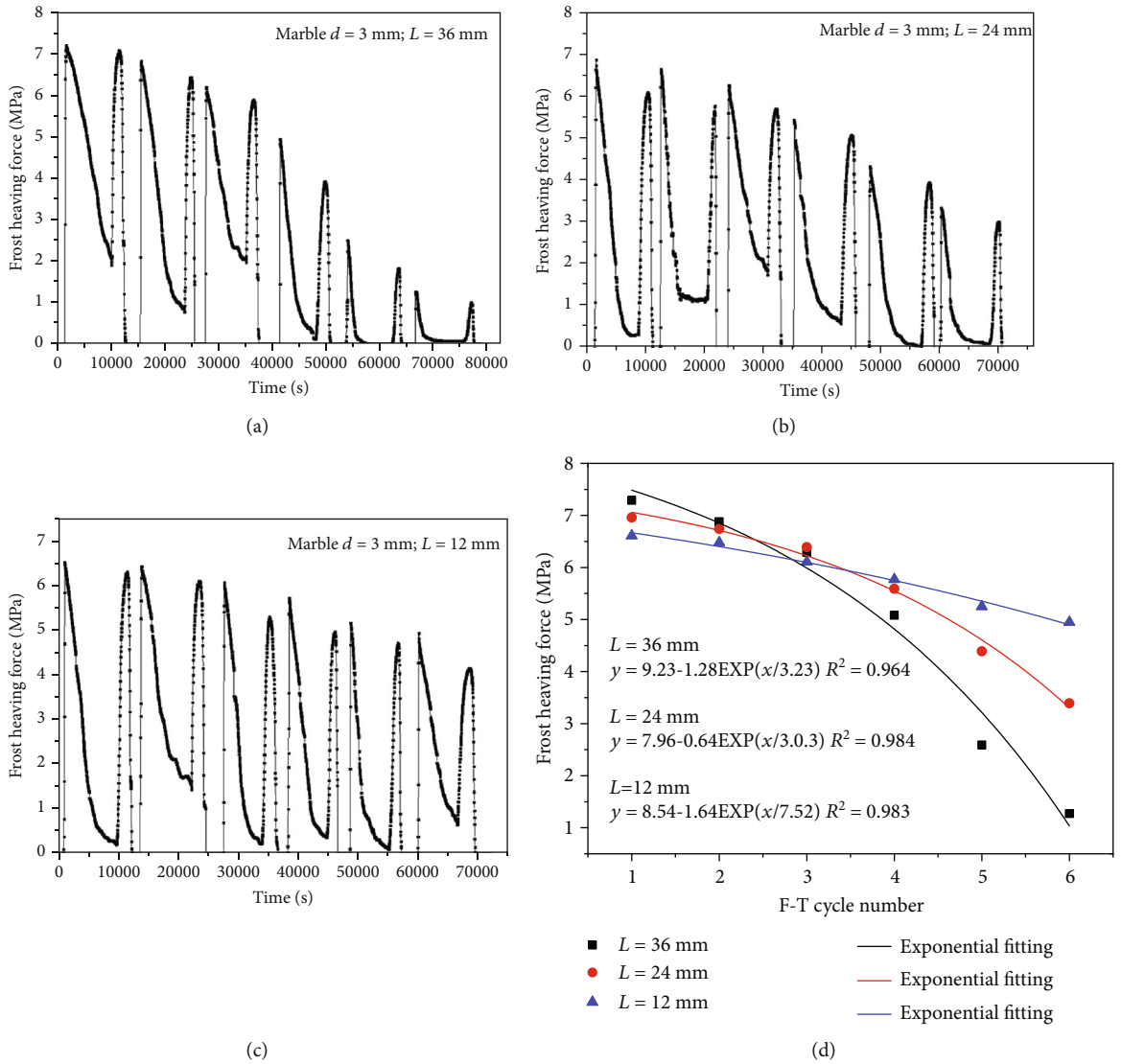

Figure 11: Optimal combinations to maximize the frost heaving force. (a–d) Plots of the optimal factors of flaw width, flaw length, flaw cement type, and rock lithology, respectively.

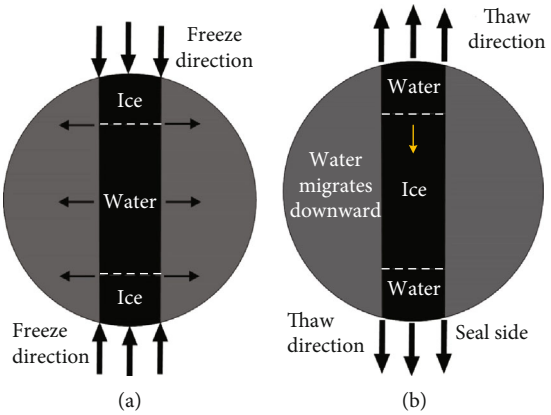

Figure 12: Water-ice phase transformation process: (a) freezing process; (b) thawing process.

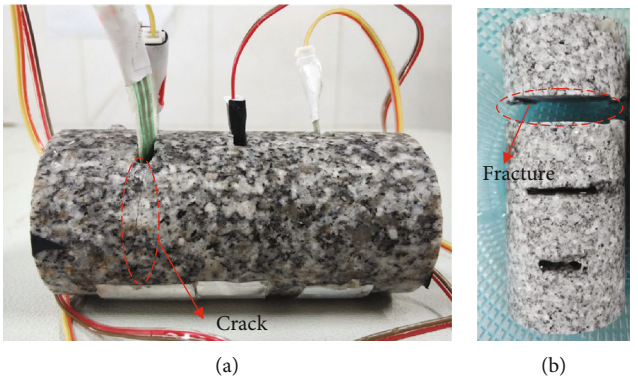

Figure 13: Formation of the frost heaving crack: (a) generation of microcrack; (b) rock fracturing.

both decrease. This implies that fatigue freeze-thaw action leads to damage in the flaw tip and even the propagation of flaws. The FHF drives the propagation of flaw and even leads to the failure of the rock sample, as shown in Figure 9(d). We can deduce that rock can be fractured if the F-T cycle number is large enough; that is to say, the damage caused by F-T treatment can accumulate until fracture of rock. The experimental results also reveal the fact that the lithology influences the tensile stress acting on rock flaws. This result is the same as the previous studies [26–31]. The mesoscopic structure of rock influences the water migration, water-ice phase transformation, and the associated FHF accumulation. Because the water storage capacity in the flaws is up to the rock permeability, the water is difficult to migrate into the rock matrix for rock having compactness texture. Therefore, enclose space in flaws is easy to be formed, and high efficiency for the germination of frost heaving force and release provides a good condition. In this work, only the two factors of flaw length and width are considered to FHF evolution; the developed degree of flaws influences the water storage capacity, the maximum FHF that can be generated, and also the ability to withstand frost heaving force. As a result, the higher the degree of the crack network in rock mass is, the greater the F-T degradation after cyclic F-T treatment is. For engineering rock mass in cold regions, rocks are often subjected to stress disturbance [32–36], and the coupled freeze-thaw action and stress disturbance should be considered simultaneously in order to evaluate the stability of rock mass objectively.

5. Conclusions

The fatigue freeze-thaw deterioration and the associated frost heaving force evolution characteristics are experimentally investigated using a self-developed frost heaving force measurement system. The influence of lithology and flaw geometry on the evolution of frost heaving force for rock subjected to cyclic F-T treatment is revealed. The main conclusions can be summarized below:

(1) Five distinct frost heaving force evolution stages are observed from the FHF curve. Rock structural deterioration caused by frost heaving force is attributed to the tensile stress acting on rock flaws. Cyclic freeze-thaw treatment leads to the damage accumulation and the final fracture of rock

(2) Frost heaving force is affected not only by flaw geometry but also by the lithology. Rock lithology determines the water migration ability and influences the water-ice phase transformation. The flaw width and length affect the water storage capacity and the volume expansion of water and the FHF accumulation

(3) The FHF decreases with increasing the F-T cycle number, and its decreasing rate becomes faster at a high F-T cycle. In addition, the decreasing trend of FHF is related to lithology; the FHF decreasing rate is larger for marble than the granite and sandstone. This is essentially attributed to the rock mesoscopic structure

(4) For hard rock with low porosity in cold regions, crack propagates quickly after the occurrence of freeze-thaw damage. It suggests that cyclic freeze-thaw treatment can finally result in the fracture of naturally fractured rock mass, if the number of the F-T cycle is large enough

Data Availability

The experimental data used to support the findings of this study are included within the article.

Conflicts of Interest

The authors declare no conflict of interest.

Acknowledgments

This research was funded by the Beijing Natural Science Foundation (8202033), the National key technologies Research and Development program (2018YFC0808402), and the Fundamental Research Funds for the Central Universities (FRF-TP-20-004A2).

References

[1] N. Matsuoka and H. Sakai, "Rockfall activity from an alpine cliff during thawing periods," *Geomorphology*, vol. 28, no. 3-4, pp. 309–328, 1999.

[2] O. Sass, "Rock moisture fluctuations during freeze-thaw cycles: preliminary results from electrical resistivity measurements," *Polar Geography*, vol. 28, no. 1, pp. 13–31, 2004.

[3] Y. J. Shen, G. S. Yang, H. W. Huang, T. L. Rong, and H. L. Jia, "The impact of environmental temperature change on the interior temperature of quasi-sandstone in cold region: experiment and numerical simulation," *Engineering Geology*, vol. 239, pp. 241–253, 2018.

[4] Y. Wang, W. K. Feng, H. J. Wang, C. H. Li, and Z. Q. Hou, "Rock bridge fracturing characteristics in granite induced by freeze-thaw and uniaxial deformation revealed by AE monitoring and post-test CT scanning," *Cold Regions Science and Technology*, vol. 177, p. 103115, 2020.

[5] N. Matsuoka, "Microgelivation versus macrogelivation: towards bridging the gap between laboratory and field frost weathering," *Permafrost and Periglacial Processes*, vol. 12, no. 3, pp. 299–313, 2001.

[6] Y. Wang, S. H. Gao, C. H. Li, and J. Q. Han, "Investigation on fracture behaviors and damage evolution modeling of freeze-thawed marble subjected to increasing- amplitude cyclic loads," *Theoretical and Applied Fracture Mechanics*, vol. 109, article 102679, 2020.

[7] M. Ishikawa, Y. Kurashige, and K. Hirakawa, "Analysis of crack movements observed in an alpine bedrock cliff," *Earth Surface Processes and Landforms*, vol. 29, no. 7, pp. 883–891, 2004.

[8] E. M. Winkler, "Frost damage to stone and concrete: geological considerations," *Engineering Geology*, vol. 5, no. 2, pp. 315–323, 1968.

[9] S. Akagawa and M. Fukuda, "Frost heave mechanism in welded tuff," *Permafrost and Periglacial Processes*, vol. 2, no. 4, pp. 301–309, 1991.

[10] D. Arosio, L. Longoni, and F. Mazza, "Freeze-thaw cycle and rockfall monitoring," in *Landslide Science and Practice*, C. Margottini, P. Canuti, and K. Sassa, Eds., pp. 385–390, Springer Verlag, Berlin, 2013.

[11] G. P. Davidson and J. F. Nye, "A photoelastic study of ice pressure in rock cracks," *Cold Regions Science and Technology*, vol. 11, no. 2, pp. 141–153, 1985.

[12] H. Lin, D. Lei, R. Yong, C. Jiang, and S. Du, "Analytical and numerical analysis for frost heaving stress distribution within rock joints under freezing and thawing cycles," *Environmental Earth Sciences*, vol. 79, no. 12, 2020.

[13] M. Bost and A. Pouya, "Stress generated by the freeze–thaw process in open cracks of rock walls: empirical model for tight limestone," *Bulletin of Engineering Geology and the Environment*, vol. 76, pp. 1491–1505, 2017.

[14] S. B. Huang, Q. S. Liu, and A. P. Cheng, "Preliminary experimental study of frost heaving pressure in crack and frost heaving propagation in rock mass under low temperature," *Rock and Soil Mechanics*, vol. 39, no. 1, pp. 78–84, 2018.

[15] Z. Lv, C. Xia, Q. Li, and Z. Si, "Empirical frost heave model for saturated rock under uniform and unidirectional freezing conditions," *Rock Mechanics and Rock Engineering*, vol. 52, no. 3, pp. 955–963, 2019.

[16] G. Zhang, G. Chen, Z. Xu, Y. Yang, and Z. Lin, "Crack failure characteristics of different rocks under the action of frost heaving of fissure water," *Frontiers in Earth Science*, vol. 8, p. 13, 2020.

[17] Y. Wang, J. Q. Han, and C. H. Li, "Acoustic emission and CT investigation on fracture evolution of granite containing two flaws subjected to freeze–thaw and cyclic uniaxial increasing-amplitude loading conditions," *Construction and Building Materials*, vol. 260, p. 119769, 2020.

[18] Y. Wang, S. H. Gao, C. H. Li, and J. Q. Han, "Energy dissipation and damage evolution for dynamic fracture of marble subjected to freeze-thaw and multiple level compressive fatigue loading," *International journal of fatigue*, vol. 142, article 105927, 2021.

[19] C. Xia, Z. Lv, Q. Li, J. Huang, and X. Bai, "Transversely isotropic frost heave of saturated rock under unidirectional freezing condition and induced frost heaving force in cold region tunnels," *Cold Regions Science and Technology*, vol. 152, pp. 48–58, 2018.

[20] J. P. McGreevy and W. B. Whalley, "Rock moisture content and frost weathering under natural and experimental conditions: a comparative discussion," *Arctic and Alpine Research*, vol. 12, no. 6, pp. 337–346, 1985.

[21] S. Huang, Q. Liu, Y. Liu, Y. Kang, A. Cheng, and Z. Ye, "Frost heaving and frost cracking of elliptical cavities (fractures) in low- permeability rock," *Engineering Geology*, vol. 234, pp. 1–10, 2018.

[22] H. Liu, X. Yuan, and T. Xie, "A damage model for frost heaving pressure in circular rock tunnel under freezing-thawing cycles," *Tunnelling and Underground Space Technology*, vol. 83, pp. 401–408, 2019.

[23] Q. S. Liu, S. B. Huang, Y. S. Kang, Y. C. Pan, and X. Z. Cui, "Experimental and theoretical studies on frost heaving pressure in a single fracture of frozen rock mass under low temperature," *Chinese Journal of Rock Mechanics and Engineering*, vol. 37, no. 9, pp. 1572–1580, 2015.

[24] H. Jia, K. Leith, and M. Krautblatter, "Path-dependent frost-wedging experiments in fractured, low-permeability granite," *Permafrost and Periglacial Processes*, vol. 28, no. 4, pp. 698–709, 2017.

[25] R. Ulusay, *The ISRM Suggested Methods for Rock Characterization, Testing and Monitoring: 2007-2014*, Springer, 2014.

[26] Z. Li, H. Liu, Z. Dun, L. Ren, and J. Fang, "Grouting effect on rock fracture using shear and seepage assessment," *Construction and Building Materials*, vol. 242, article 118131, 2020.

[27] Y. Wang, C. Li, J. Han, and H. Wang, "Mechanical behaviours of granite containing two flaws under uniaxial increasing amplitude fatigue loading conditions: an insight into fracture evolution analyses," *Fatigue and Fracture of Engineering Materials and Structures*, vol. 43, no. 9, pp. 2055–2070, 2020.

[28] Z. Li, H. Zhou, D. Hu, and C. Zhang, "Yield criterion for rock-like geomaterials based on strain energy and CMP model," *International Journal of Geomechanics*, vol. 20, no. 3, article 04020013, 2020.

[29] Y. Wang, B. Zhang, S. H. Gao, and C. H. Li, "Investigation on the effect of freeze-thaw on fracture mode classification in marble subjected to multi-level cyclic loads," *Theoretical and Applied Fracture Mechanics*, vol. 111, article 102847, 2021.

[30] Z. Li, S. Liu, W. Ren, J. Fang, Q. Zhu, and Z. Dun, "Multiscale laboratory study and numerical analysis of water-weakening effect on shale," *Advances in Materials Science and Engineering*, vol. 2020, Article ID 5263431, 14 pages, 2020.

[31] Q. Meng, H. Wang, M. Cai, W. Xu, X. Zhuang, and T. Rabczuk, "Three-dimensional mesoscale computational modeling of soil-rock mixtures with concave particles," *Engineering Geology*, vol. 277, article 105802, 2020.

[32] C. Zhu, X. D. Xu, X. T. Wanget al. et al., "Experimental investigation on nonlinear flow anisotropy behavior in fracture media," *Geofluids*, vol. 2019, Article ID 5874849, 9 pages, 2019.

[33] C. Zhu, M. C. He, M. Karakus, X. B. Cui, and Z. G. Tao, "Investigating toppling failure mechanism of anti-dip layered slope due to excavation by physical modelling," *Rock Mechanics and Rock Engineering*, vol. 53, no. 11, pp. 5029–5050, 2020.

[34] Y. Wang, W. K. Feng, and C. H. Li, "On anisotropic fracture and energy evolution of marble subjected to triaxial fatigue cyclic-confining pressure unloading conditions," *International Journal of Fatigue*, vol. 134, p. 105524, 2020.

[35] Y. Wang, S. Gao, D. Liu, and C. Li, "Anisotropic fatigue behaviour of interbeded marble subjected to uniaxial cyclic compressive loads," *Fatigue & Fracture of Engineering Materials & Structures*, vol. 43, no. 6, pp. 1170–1183, 2020.

[36] Y. Wang, D. Q. Liu, J. Q. Han, C. H. Li, and H. Liu, "Effect of fatigue loading-confining stress unloading rate on marble mechanical behaviors: an insight into fracture evolution analyses," *Journal of Rock Mechanics and Geotechnical Engineering*, vol. 12, no. 6, pp. 1249–1262, 2020.